Journal of Thermal Analysis and Calorimetry (2019) 138:3267–3276
https://doi.org/10.1007/s10973-019-08612-y

Mechanical and thermal properties of fly ash-filled geopolymers

Michelina Catauro[1] · Elisabetta Tranquillo[1] · Federico Barrino[1] · Giovanni Dal Poggetto[2] · Ignazio Blanco[3,4] · Gianluca Cicala[3,4] · Giulia Ognibene[3,4] · Giuseppe Recca[5]

Received: 22 March 2019 / Accepted: 19 July 2019 / Published online: 2 August 2019

Abstract
Fly ash recycling reduces the amount of waste to be treated or disposed in landfills, allowing both to decrease the environmental damage and to save the costs of transport and disposal of waste. Systems with different percentages in mass of fly ash (20, 50 and 70 mass%) and the remaining part of pure metakaolin were synthesized. The effect of fly ash on the mechanical and thermal properties of a new geopolymer has been investigated in this paper. Fourier transform infrared spectroscopy has allowed us to verify the bonds formation between the geopolymeric matrix and the fly ash. The consolidation of the materials has been confirmed by pH and conductivity at up to 28 days of hardening. Dynamic mechanical analysis, differential scanning calorimetry and thermogravimetric analysis were performed in order to evaluate the thermo-mechanical performance of this new geopolymer in comparison with its counterpart pure geopolymer.

Keywords Fly ash · Geopolymers · FTIR · Thermal analysis

Introduction

Geopolymers are synthetic inorganic polymers based on aluminosilicate or phosphate, dissolved in a strongly basic environment, produced according to a process defined as geopolymerization [1, 2]. Geopolymers can be considered ceramics consolidated by alkaline reaction as they respect the chemical and mechanical properties of ceramics [3, 4]. These materials are composite, consisting of a geopolymeric resin that acts as a glue for inert resources, thus improving chemical properties by functionalizing and reinforcing the reactive inorganic raw materials, in particular metakaolines [5]. Geopolymers are produced by molding without the use of additional finishes and used in many sectors such as construction, waste treatment, synthesis of biomaterials, [6–8]. Waste and industrial by-products of various kinds can be recycled as raw materials or inert fillers for this type of application at low processing temperatures, reducing production prices, thus making geopolymers eco-friendly and eco-sustainable materials [9]. Geopolymers can be exposed to high heat sources, due to a great tolerance to high temperatures because they are non-combustible, they do not develop gas or fumes, they are not toxic and do not explode as, contrary to traditional hydraulic cements, they do not contain water in structure. In recent years, these inorganic polymers have attracted growing attention because they have performances comparable to those of Portland cement, but are able to reduce CO_2 emissions [10, 11]. Metakaolin (MK) is unique as it is the only entirely natural supplementary cementitious material, which is not a by-product of an industrial process. It is obtained by calcination of kaolin clays, a hydrated aluminosilicate mineral clay.

The aim of this work is to create a composite geopolymer using fly ash recycling in order to reduce the amount of waste to be treated or disposed in landfills, allowing both to decrease the environmental damage and to

✉ Michelina Catauro
michelina.catauro@unicampania.it

1 Department of Engineering, University of Campania "Luigi Vanvitelli", Via Roma 29, 81031 Aversa, Italy

2 Ecoricerche Srl, Via Principi Normanni 36, 81043 Capua, Italy

3 Department of Civil Engineering and Architecture, University of Catania, Viale Andrea Doria 6, 95125 Catania, Italy

4 UdR-Catania Consorzio INSTM, University of Catania, Viale Andrea Doria 6, 95125 Catania, Italy

5 Institute for Polymers, Composites and Biomaterials (ICPB), National Research Council (CNR), Via Paolo Gaifami 17, 95125 Catania, Italy

save the costs of transport and disposal of waste. New compounds, with improved physical and chemical properties, based on metakaolin with different percentages of flying ash (20, 50 and 70 mass%) were synthesized through the geopolymerization process in order to recycle waste materials. Fourier transform infrared spectroscopy (FTIR) and energy-dispersive X-ray fluorescence (ED-XRF) analysis was performed to follow the structural modification of the materials induced by the addition of ash. Thermo-mechanical analysis, namely dynamic mechanical analysis (DMA), differential scanning calorimetry (DSC) and thermogravimetric analysis (TGA), was carried out to study the variation of physical properties of the prepared materials as a function of temperature.

Experimental

Materials

The kaolinite was calcinated at 700 °C for 4 h and then ground and sieved to < 70 μm, obtaining the metakaolin (MK) that was used as aluminosilicate precursor. In order to prepare an alkaline solution, the sodium silicate solution was used; it is a viscous liquid produced for the cement industry (Ingessil, Verona, Italy) with molar $SiO_2/Na_2O = 3$ and mass ratio = 2.89 (26.45 mass% of SiO_2 and 9.14 mass% of Na_2O), as well as a density of 1.38 g cm^{-3} and 39.44 Baume scales. The sodium hydroxide solution was obtained by dissolving pellets (99.6 mass%, Carlo Erba, Italy) in distilled water to reach 8 M concentration. The fly ashes were obtained by the calcination process of the glass processing scraps, which are used as source materials.

Synthesis method

After the glass working process, the waste that is obtained is not dry, having a consistency similar to that of mud because they are rich in H_2O. In order to completely remove the water from these scraps, the mud was dried in a stove at 100 °C for 24 h. The ash obtained was ground in a fast laboratory ball mill and sieved through 110- and 30-μm filters in order to evaluate the effect of grain size [12–14]. Different percentages of fly ash (20, 50 and 70 mass%) and the last part of pure metakaolin were used to prepare the several geopolymers. This powder was subjected to alkaline activation, using a strongly basic solution consisting of sodium silicate (26.5 mass% SiO_2, 10.6 mass% Na_2O, 62.9 mass% H_2O) in which NaOH pellets have been dissolved. The formulation of mixtures was designed to obtain Si/Al and Na/Al ratios of 2.16 and 1.01, respectively. The dough was poured into plastic molds, and the consolidation phase carried out at 50 °C for 24 h; the hardening phase was carried out at room temperature for 7, 14 and 28 days. This last curing time was investigated for samples containing glass with a fine grain size only. The whole process of synthesis is illustrated in Fig. 1.

Chemical, spectroscopic and structural characterization

The chemical structure of the synthesized powders was investigated by Fourier transform infrared spectroscopy using a Prestige 21 Shimadzu (Kyoto, Japan) instrument equipped with a DTGS detector, used to study the interactions between the different components. The spectra of the materials were recorded in the 400–4000 cm^{-1} region, with resolution of 4 cm^{-1} (45 scans), by using KBr pelletized disks containing 2 mg of each sample and 198 mg of KBr. The FTIR spectra were then processed by Prestige software (IR solution, software version 1.50, Shimadzu, Kyoto, Japan).

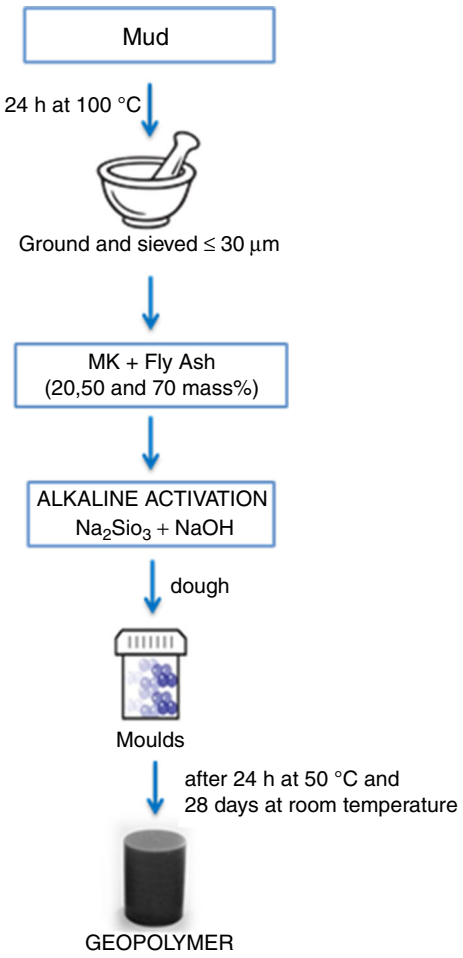

Fig. 1 Flowchart of synthesis

The chemical composition of the materials was ascertained by means of energy-dispersive X-Ray fluorescence spectroscopy using a Shimadzu energy-dispersive X-Ray fluorescence spectrometer EDX-720 equipped with 50 W Rh target X-ray tube, a high-energy resolution Si(Li) detector and five primary X-ray filters.

The solid residues obtained from the thermal analysis were investigated by FTIR using a Perkin-Elmer Spectrum 100 spectrometer with an universal ATR sampling accessory. Spectra were recorded at r.t. from 600 to 4000 cm^{-1}, with a resolution of 4.0 cm^{-1}, directly on compounds, without any preliminary treatment.

Microstructural analysis

The geopolymer powders were analyzed, as produced after alkaline activation, with a SEM EVO (EVO-SEM, Zeiss, Cambridge, UK). All of the samples were gold-sputtered up to a thickness of 20 nm by means of an Emitech K-550 sputter coater (Ashford Kent, UK). An accelerating voltage of 15 kV was used to collect the micrographs.

pH and conductivity analysis

In order to indirectly evaluate ion release from the different materials, pH and conductivity analysis were carried out in water, with a solid/liquid ratio of 1/10, over a period of 24 h under stirring.

Chemical analysis of fly ash and eluates

The chemical analysis of glasses was performed by inductively coupled plasma atomic emission spectroscopy (ICP-AES Varian Liberty 200). The sample was dissolved in HNO_3 solution. The metal content of all samples was investigated by microwave-assisted wet digestion using a 3:1 mixture of HNO_3 and HCl. The determination was made using an inductively coupled plasma emission spectrometer (ICPE-9000 Shimadzu, Tokyo, Japan).

Thermal analysis

Dynamic mechanical analysis was carried out on a dynamic mechanical thermal analyzer (TRITEC2000 by Triton Technology, Leicestershire, United Kingdom) by single cantilever geometry. The geopolymers, after 28 days of hardening, were tested in their powder form using the pocket DMA approach, a technique used for testing powders in the pharmaceutical field [15] and for polymer blends [16]. The geopolymers obtained from the syntheses were finely micronized in powder with an average dimension of 30 μm. Then 0.35 g of geopolymer powder was weighted in a standard stainless steel pocket purchased from Triton and pressed to obtain a uniform thickness. The test was carried out according to the following protocol: The sample was stabilized at 25 °C and then heated up to 210 °C at 5 °C min^{-1}; the samples were cooled down naturally and re-heated up to 210 °C at 5 °C min^{-1}. Similar techniques were also reported by Carlier et al. [17] for organic polymers under the name supported DMA. This kind of technique allows for direct evaluation of thermal transitions from E' and tan δ traces. However, the absolute values of E' and tan δ for the polymer are influenced by the presence of the metal pocket, and thus, the real values should be analyzed out considering the assembly as a sandwich material. The tan δ versus temperature was plotted.

A Shimadzu DSC-60 (Kyoto, Japan) was used for the calorimetric investigation. The enthalpy and temperature calibrations of the equipment were made according to a well-established procedure [18]. Samples of about 6.0×10^{-3} g, held in sealed aluminum crucibles, and a heating rate of 10 °C min^{-1} were used for measurements. Two consecutive DSC scans were carried out for each sample; the first one starting from r.t. up to 250 °C, while the second one starting from r.t. up to 400 °C.

A Shimadzu DTG-60 simultaneous DTA-TG apparatus (Kyoto, Japan) was used for thermogravimetric analysis. Temperature, heat flow and mass calibrations were carried out following the procedure suggested by Shimadzu and reported elsewhere [19]. Geopolymer samples of about 12×10^{-3} g, placed in a 40 μL alumina open pan, were used for the thermal degradations. TGA scans were carried out in the temperature range 30–800 °C, in inert (flowing nitrogen 0.02 L min^{-1}) and oxidative environment (static air), by setting a heating rate of 10 °C min^{-1}. In order to correct the error in the mass determination due to the reduction in the buoyant force with increasing temperature, we adopted the blank method suggested by the ICTAC Kinetics Committee [20]. The sample mass was then recorded as a function of the temperature and reported as the percentage of un-degraded sample, $(1 - D)\%$, where $D = (W_0 - W)/W_0$, and W_0 and W were the masses at the starting point and during scanning.

All the values, considered in this work, were averaged from those of three runs, with a maximum difference between the average and the experimental values within ± 1 °C.

Results and discussion

Spectroscopic and structural characterization

FTIR spectra of geopolymers at different content of fly ash are reported in Fig. 2 together with those of pure fly ash

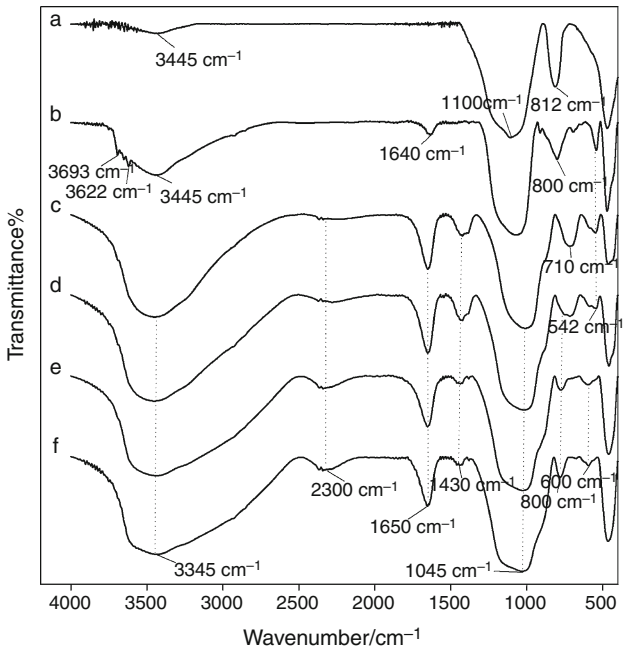

Fig. 2 Representative FTIR spectra of (a) fly ash, (b) pure metakaolin, (c) GPMK, (d) MK/$FA_{20\ mass\%}$, (e) MK/$FA_{50\ mass\%}$, (f) MK/$FA_{70\ mass\%}$

Table 1 Chemical composition (mass%) of (MK) pure metakaolin; (*C*0) GPMK; (*C*1) MK/$FA_{20\ mass\%}$; (*C*2) MK/$FA_{50\ mass\%}$; (*C*3) MK/$FA_{70\ mass\%}$

	MK	*C*0	*C*1	*C*2	*C*3
Al_2O_3	41.93	46.29	40.95	35.77	30.22
SiO_2	52.90	53.71	59.05	64.23	69.78
K_2O	0.83	0.45	0.41	0.11	<0.01
Fe_2O_3	1.15	1.01	0.92	0.87	0.79
TiO_2	1.70	1.55	1.31	0.98	0.34
MgO	0.15	0.13	< 0.01	< 0.01	< 0.01
CaO	0.10	0.81	< 0.01	< 0.01	< 0.01

and metakaolin. The bands at 3445 and 1640 cm^{-1}, due to –OH stretching and bending vibrations, change position and shape for the formation of hydrogen-bonded solvent molecules (H_2O) and hydrogen-bonded –OH groups related to Si atoms [21–23]. In particular, bending –OH vibration band at 1640 cm^{-1} in pure metakaolin spectra (curve *b*) was displaced by about 10 cm^{-1} (1650 cm^{-1}) both in the hybrids spectra. Furthermore, in all spectra are present the typical peaks of silica matrix and polymer. The asymmetric Si–O stretching and symmetric Si–O stretching are observed at 1045 cm^{-1} with a shoulder at 1100 cm^{-1}. The spectra (*b*, *c*, *d*, *e* and *f*) present the strongest vibration typical of aluminosilicates, which are assigned to internal vibrations of Si–O-Si and Si–O-Al, and an approximate relationship between the frequency of the absorption bands

Table 2 Chemical analysis test (expressed in mg L^{-1}) of fly ash; (*C*0) GPMK; (*C*1) MK/$FA_{20\ mass\%}$; (*C*2) MK/$FA_{50\ mass\%}$; (*C*3) MK/$FA_{70\ mass\%}$

	Fly ash	*C*0	*C*1	*C*2	*C*3
Al	15	44,236	27,428	19,362	9856
As	14.4	2.9	2.0	2.21	2.9
B	2.7	5.25	7.4	5.5	1.9
Ba	6.6	6.2	3.0	2.8	2.5
Be	3.7	2.5	1.1	1.5	1.8
Cd	2.3	0.5	0.9	1.4	1.9
Co	4.5	2.6	2.5	3.2	3.8
Cr	47.5	10.5	15.4	21.9	27.9
Fe	69	888	729	472	147
Mn	5.5	9.4	5.4	4.9	4.2
Mo	12.4	3.3	2.0	2.4	2.9
Ni	4.6	1.3	1.9	2.2	3.9
Pb	63.5	7.8	16.0	19.3	26.7
Sb	0.01	0.6	0.4	0.3	0.2
Se	1.5	2.6	1.2	1.0	0.9
Sn	27	5.9	5.2	5.4	6.6
V	10.4	87.1	34.4	15.0	9.8
Zn	20.1	13.9	9.8	12.3	15.1
Si	915,650	120,525	217,136	767,903	845,612

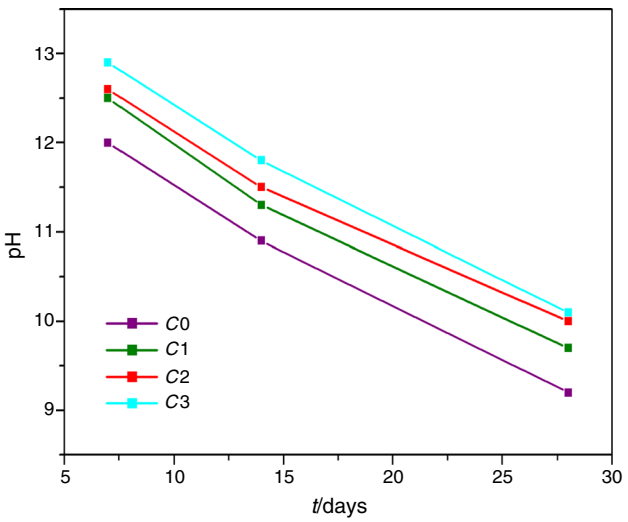

Fig. 3 Representative pH curve of (*C*0) GPMK; (*C*1) MK/$FA_{20\ mass\%}$; (*C*2) MK/$FA_{50\ mass\%}$; (*C*3) MK/$FA_{70\ mass\%}$

and the ratio of Si/Al in the alluminosilicate framework was observed: The higher the Al inclusions, the lower the wavelength [24–26]. The spectrum of MK also revealed sharp peaks in the range 3622–3693 cm^{-1}, ascribed to the stretching of hydroxyl groups and of Al(VI)–OH bonds in the kaolinite residues [27]. The presence of the band around 800 cm^{-1} (curve *b*), due to the stretching of the Al(IV), is also visible in the spectra *d*, *e* and *f* with

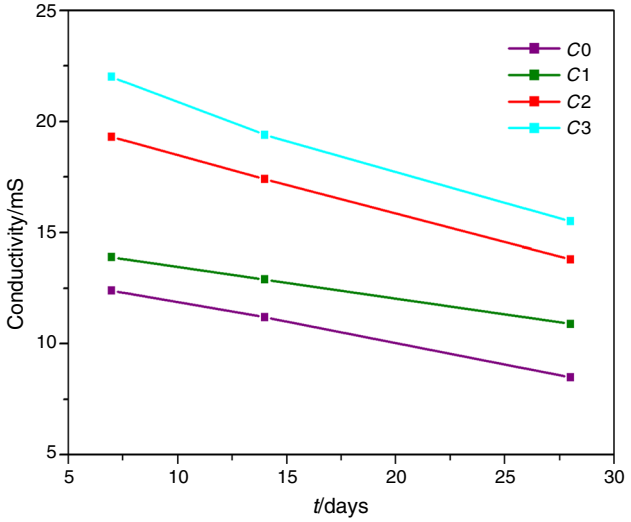

Fig. 4 Representative conductivity curve of (*C*0) GPMK; (*C*1) MK/$FA_{20\ mass\%}$; (*C*2) MK/$FA_{50\ mass\%}$; (*C*3) MK/$FA_{70\ mass\%}$

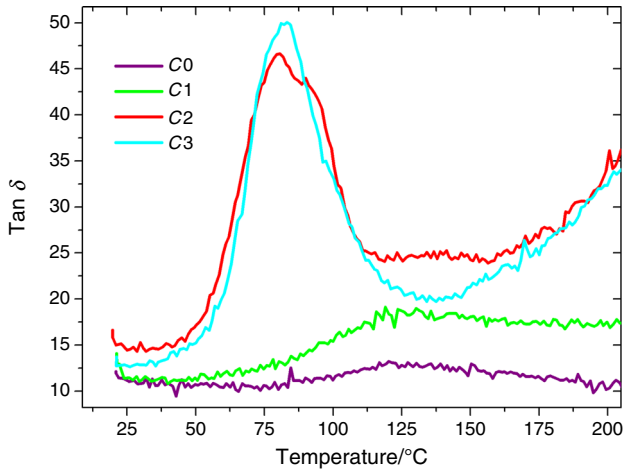

Fig. 5 DMA curves of (*C*0) GPMK; (*C*1) MK/$FA_{20\ mass\%}$; (*C*2) MK/$FA_{50\ mass\%}$; (*C*3) MK/$FA_{70\ mass\%}$

decreasing intensity. Even the typical sodium carbonate group at 1430 cm^{-1}, very intense in the curve c and *d*, decreases as the percentage by mass of the built-in flying ash increases (curve *e* and *f*). That is due to the passage of water through the bulk during the drying of the sample, which generates a high concentration of sodium close to the surface, where it forms carbonates after the reaction with atmospheric CO_2.

The chemical composition of the powders and their purity have been asserted by the analysis and XRF, and the results are summarized in Table 1. No impurities were detected in the powders obtained after the geopolymerization process, while in the MK there were natural impurities, even if in small quantities. The color of the powders confirmed the result of the analysis XRF: MK was

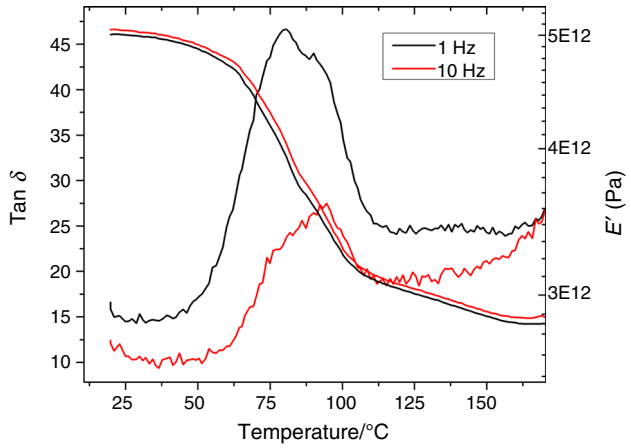

Fig. 6 DMA curves of $MK/FA_{50\ mass\%}$ (C2) tested at 1 and 10 Hz

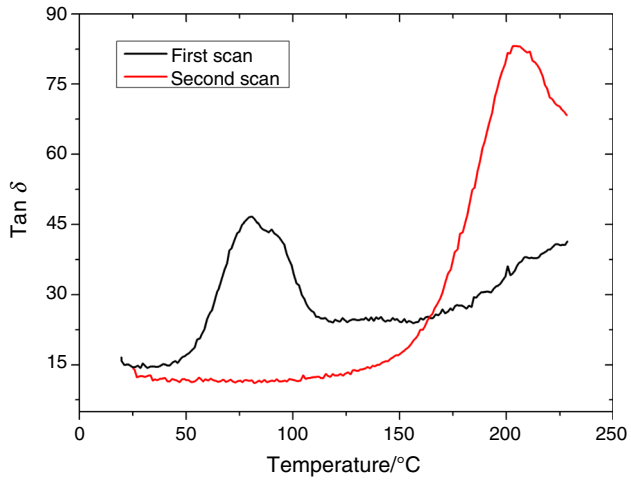

Fig. 7 DMA curves of (C2): first heating scan vs second heating scan

pinkish (mainly because of the presence of Fe_2O_3), while all the powders were light gray.

The chemical analysis (Table 2) of all samples was evaluated by ICP analysis. The results of chemical analysis (Table 2) confirmed that the fly ash was rich in Si. In geopolymers, the metals diminish as the percentage of fly ash increases. These metals have been incorporated into the materials. For this reason, the materials obtained with the geopolymerization are less toxic than the raw materials used.

Chemical characterization

The geopolymerization process of all samples was evaluated as a function of the polymerization time, using pH and conductivity analysis. Figure 3 shows that as the polymerization time increases, the pH decreases. This result is due to the decrease in free ions in the network, corresponding to a higher degree of geopolymerization [28]. For

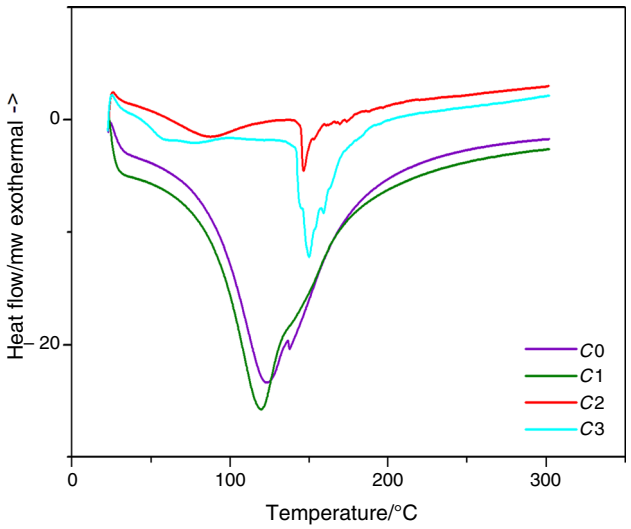

Fig. 8 DSC curves, for the first heating, of (*C*0) GPMK; (*C*1) MK/$FA_{20\ mass\%}$; (*C*2) MK/$FA_{50\ mass\%}$; (*C*3) MK/$FA_{70\ mass\%}$

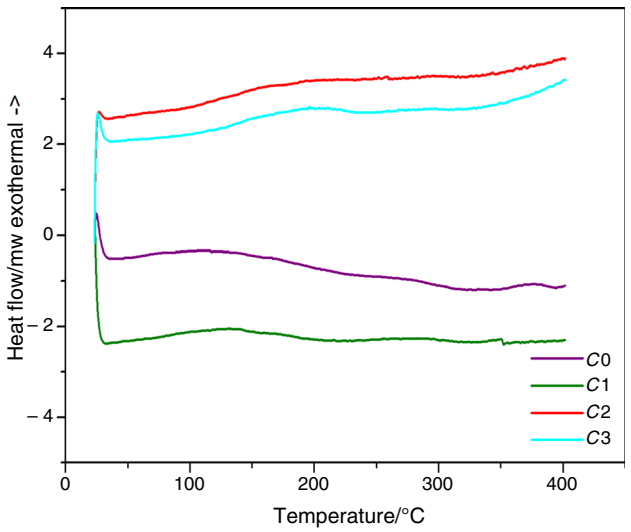

Fig. 9 DSC curves, for the second heating (after cooling), of (*C*0) GPMK; (*C*1) MK/$FA_{20\ mass\%}$; (*C*2) MK/$FA_{50\ mass\%}$; (*C*3) MK/$FA_{70\ mass\%}$

all synthesized materials, the results are confirmed. In the geopolymers containing a large percentage by mass of fly ash, it is possible to observe the slight increase in the initial pH, followed by a similar decrease in the samples with a lower percentage by mass of fly ash, which occurs as a function of the aging time. This suggests that the composition of raw materials affects the properties of the geopolymer. The different behavior of the samples containing a high percentage by mass of fly ash is also evidenced by the conductivity values. In fact, from Fig. 4 lower values of conductivity are observed when the built-in

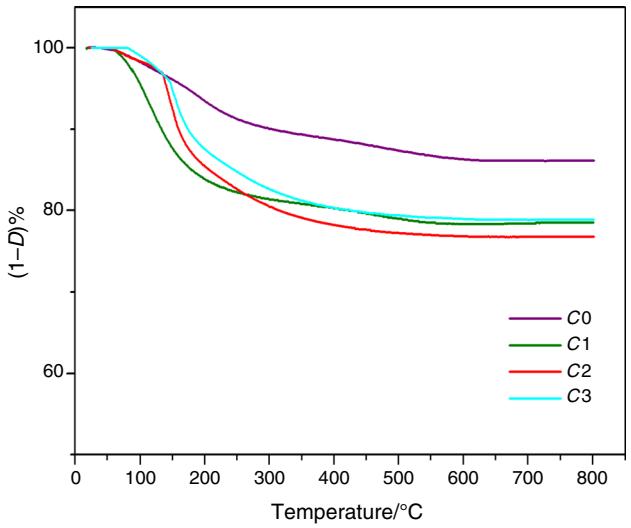

Fig. 10 TGA curves, in flowing nitrogen atmosphere, of (*C*0) GPMK; (*C*1) MK/$FA_{20\ mass\%}$; (*C*2) MK/$FA_{50\ mass\%}$; (*C*3) MK/$FA_{70\ mass\%}$

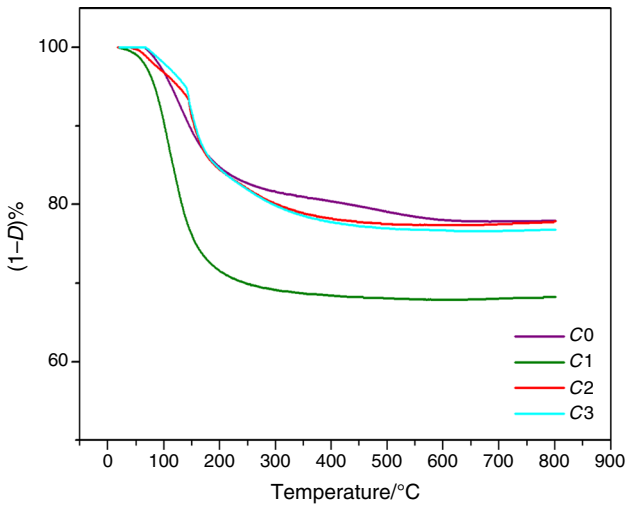

Fig. 11 TGA curves, in static air atmosphere, of (*C*0) GPMK; (*C*1) MK/$FA_{20\ mass\%}$; (*C*2) MK/$FA_{50\ mass\%}$; (*C*3) MK/$FA_{70\ mass\%}$

fly ash decreases. These results are due to the smaller amount of ions in the eluted solution.

Thermal analysis

All the samples were tested under oscillatory mode while heating from 25 to 210 °C at 5 °C min^{-1}. The results, from the first heating scan, are summarized in Fig. 5. The samples C2 and C3 show a clear tan δ peak centered between 75 and 85 °C, while the formulations C0 and C1 show a smoother tan δ peak at about 110–125 °C. Figure 6 shows the tan δ behavior for the formulation C2 tested at two different frequencies (1 and 10 Hz). The tan δ showed a shift to higher temperature when tested at 10 Hz rather

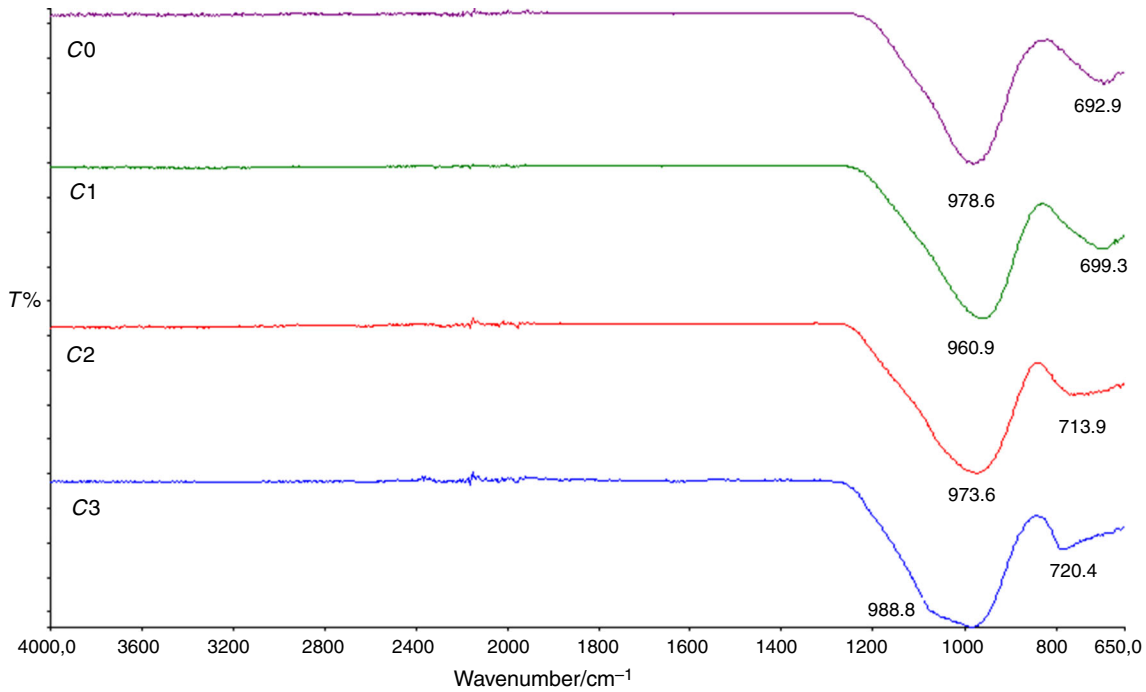

Fig. 12 FTIR spectra of the residues, obtained at 800 °C in flowing nitrogen, of (*C*0) GPMK; (*C*1) MK/$FA_{20\ mass\%}$; (*C*2) MK/$FA_{50\ mass\%}$; (*C*3) MK/$FA_{70\ mass\%}$

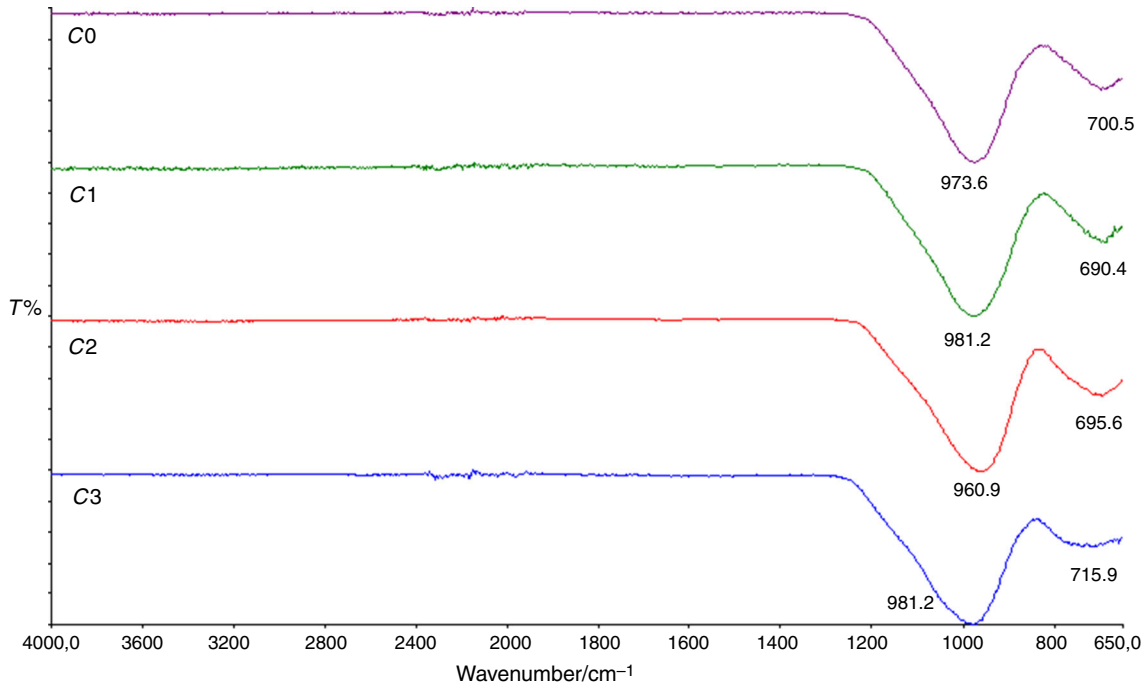

Fig. 13 FTIR spectra of the residues, obtained at 800 °C in static atmosphere, of (*C*0) GPMK; (*C*1) MK/$FA_{20\ mass\%}$; (*C*2) MK/$FA_{50\ mass\%}$; (*C*3) MK/$FA_{70\ mass\%}$

than 1 Hz. This behavior is usually observed for relaxation phenomena like glass transition observed in polymers [29, 30]. The storage modulus (*E*') showed a clear decay starting from 50 °C. Similar behavior is shown by polymers when relaxation phenomena like glass transition occur. The sample analyzed was hardened at room temperature for 28 days; therefore, the transitions measured by

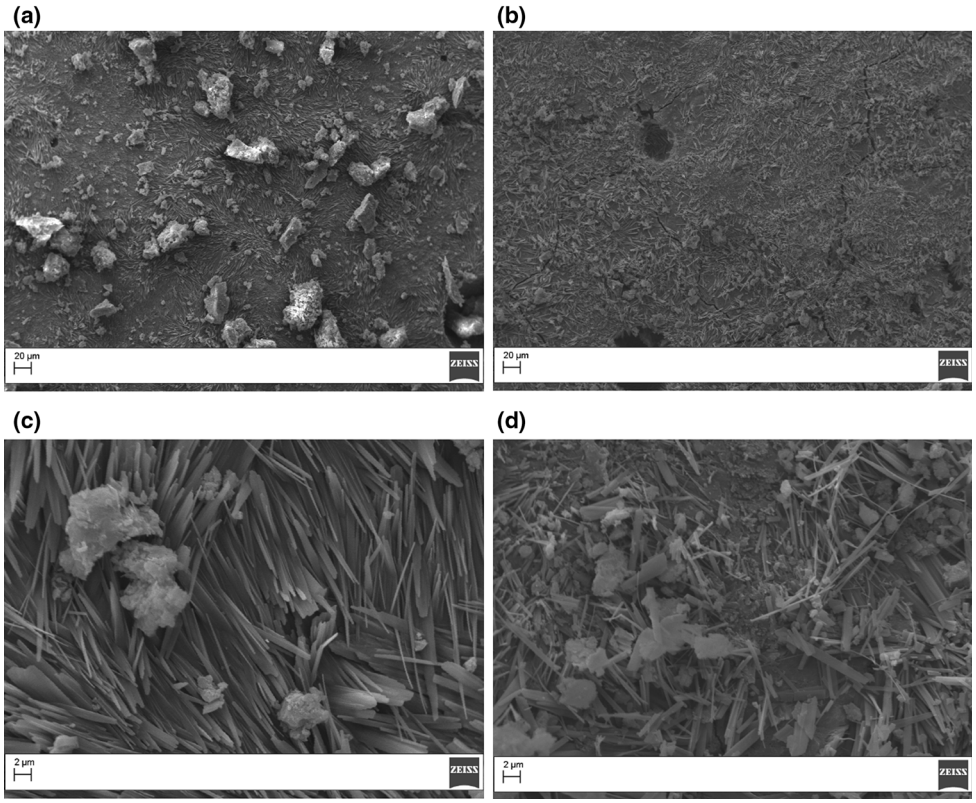

Fig. 14 SEM analysis of (C0) GPMK on the left; (*C*1) MK/$FA_{20\ mass\%}$ on the right: low magnification (500 ×) up; high magnification (5000 ×) down

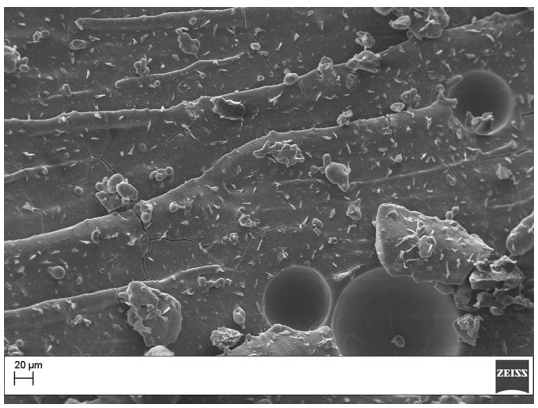

Fig. 15 SEM analysis of (*C*3) MK/$FA_{70\ mass\%}$ (magnification 500 ×)

DMA can be explained as devitrification of the curing network which is formed during hardening [31].

The sample C2, after cooling at room temperature, was analyzed with a second ramp temperature and the tan δ peak shifted to 205 °C (Fig. 7). After the first heating, the sample displayed a clear increase in the transition peak. This behavior is because of the structural changes occurring during the hardening reaction induced by the heat increases, and it is the result of the partial curing that occurred on the sample hardened at room temperature only. Similar behavior was observed by *C*3 formulation, while *C*0 and *C*1 formulations did not display such a clear change in the temperature range analyzed. As reported by Rahier et al. [32], the geopolymer mixtures follow a polymerization route that resembles the curing of organic thermosets.

DSC analysis seems to confirm the behavior observed during the dynamic mechanical analysis. Apart from a peak due to the mass loss caused by the presence of structural water in the geopolymer composition [33], that was less intense and shifted to lower temperature by increase in the fly ash content in the formulation, *C*2 and *C*3 samples showed a clear irreversible endothermic phenomenon at 147 and 150 °C, respectively (Fig. 8). The same phenomena, at slight lower temperature, for *C*0 and *C*1 samples were probably covered by the water loss, as testified by the shoulder present in the main peak at 138 and 140 °C, respectively. A second scan was carried out for each geopolymer, after cooling, that confirm the irreversible nature of the endothermic transition and confirm the presence of the relaxation phenomena at higher temperatures (Fig. 9) with the same trend, namely 179, 186, 205 and 207 °C for samples *C*0, *C*1, *C*2 and *C*3, respectively.

Finally, thermogravimetric analysis was carried out, both for evaluating the resistance to the thermal degradation of these materials and for confirming that the DSC peaks around 100 °C can be attributed to mass (water) loss. TGA degradation was carried out in inert (nitrogen flow) (Fig. 10) and oxidative (static air) (Fig. 11) atmospheres, confirming the start of mass loss with the values of the first endothermic DSC peak in both investigated environments. After this degradation, the TGA curve proceeds without further mass loss and the formation of a stable residue remains constant in mass up to 800 °C, testifying the great thermal resistance of these materials. The stable residue, as expected, decreases with the increase in ash content in the formulation. The residues derived from the degradation at 800 °C were analyzed by FTIR spectroscopy, and the corresponding spectra are reported in Figs. 12 and 13. No differences in the residues of the different geopolymers have been found, showing all the investigated samples IR bands at about 960–980 and 700 cm^{-1} to be attributable to the presence of silica [34, 35].

Scanning electron microscopy (SEM) analysis

The hardened geopolymers (28 days) were analyzed by SEM. The sample *C*0 shows a uniform distribution of lamellar structures longer than 5 μm, and some granular structures with sizes variable from 5 to 20 μm (Fig. 14). The sample *C*1 shows the lamellar structures but smaller granular structures than the sample *C*0 as a result of the fly ash addition. Lamellar structures similar to those observed here are reported in the literature [36, 37]. With the increase in the amount of fly ash content the lamellar structure is reduced and the sample appears more compact (Fig. 15).

Conclusions

Geopolymerization is a possible technology for the management of large amount of potentially hazardous or abundant wastes. In particular, waste glass, obtained from the glass processing, acts as filler, not showing high reactivity in the geopolymeric matrix but also not hindering the geopolymerization of the matrix. After 28 days at room temperature, the samples synthesized using different percentages in mass of fly ash showed a good geopolymerization. This was confirmed by the FTIR analysis, which showed the formation of bonds between both components. The reduction of free ions in the network as the drying period increases was demonstrated with a decrease in the pH value and conductivity. The chemical composition, analyzed with ICP and XRF, highlighted the great presence of silicates in fly ash and metakaolin alumina. The geopolymers showed a proportional mixed composition.

The transitions observed by DMA were attributed to the devitrification of the curing network, which is formed during hardening at room temperature for 28 days. These results were also confirmed by DSC analysis that suggest the irreversible nature of the endothermic transition and confirm the presence of the relaxation phenomena at higher temperature in all samples.

Finally, to evaluate the resistance to the thermal degradation and to confirm the mass (water) loss observed in DSC analysis, thermogravimetric analysis was carried out. Furthermore, the residues derived from the degradation at 800 °C were analyzed by FTIR spectroscopy, showing the same nature for all the samples attributable to the presence of silica.

The SEM analysis showed us a reduction in the length of the lamellae with the increase in incorporated fly ash, thus demonstrating a greater compactness of the sample.

Although the results may show a potential use of these compounds containing different percentages of fly ash as building materials, future analyses will be carried out to evaluate their mechanical properties as well.

References

1. Takeda H, Hashimoto S, Kanie H, Honda S, Iwamoto Y. Fabrication and characterization of hardened bodies from Japanese volcanic ash using geopolymerization. Ceram Int. 2014;40(3):4071–6.
2. Siyal AA, Azizli KA, Man Z, Ismail L, Khan MI. Geopolymerization kinetics of fly ash based geopolymers using JMAK model. Ceram Int. 2016;42(14):15575–84.
3. Davidovits J. Geopolymers. J Therm Anal. 1991;37(8):1633–56.
4. Bai C, Colombo P. Processing, properties and applications of highly porous geopolymers: a review. Ceram Int. 2018;44(14):16103–18.
5. Zhang F, Zhang L, Liu M, Mub C, Liang YN, Hu X. Role of alkali cation in compressive strength of metakaolin based geopolymers. Ceram Int. 2017;43(4):3811–7.
6. Guimarães Oliveira Grance E, das Dores Macedo Paiva M, de Souza Junior FG, Dias Toledo Filho R. Geopolymer: a review of structure, applications and properties of fiber reinforced composites. Research & Development in Material Science. 2018;7(4):1–8.
7. Provis JL, Van Deventer JSJ, editors. Geopolymers: structures processing, properties, and industrial applications. New York: Elsevier; 2009.
8. Davidovits, J. (2002) Years of successes and failures in geopolymer applications. Market trends and potential breakthroughs. In: Geopolymer 2002 Conference (Vol. 28, p. 29). Geopolymer Institute Saint-quentin (France), Melbourne (Australia).
9. Singh B, Ishwarya G, Gupta M, Bhattacharyya SK. Geopolymer concrete: a review of some recent developments. Constr Build Mater. 2015;85(15):78–90.

10. Hardjito D, Wallah SE, Sumajouw DMJ, Rangan BV. On the development of fly ash-based geopolymer concrete. Mater J. 2014;101(6):467–72.
11. Samal S, Kolinova M, Rahier H, Dal Poggetto G, Blanco I. Investigation of the internal structure of fiber reinforced geopolymer composite under mechanical impact: a micro computed tomography (μCT) study. Appl Sci. 2019;9(3):516.
12. Qian G, Yang X, Dong S, Zhou J, Sun Y, Xu Y, Liu Q. Stabilization of chromium-bearing electroplating sludge with MSWI fly ash-based Friedel matrices. J Hazard Mater. 2009; 165(1–3):955–60.
13. Lancellotti I, Ponzoni C, Barbieri L, Leonelli C. Alkali activation processes for incinerator residues management. Waste Manag. 2013;33(8):1740–9.
14. Lancellotti I, Ponzoni C, Bignozzi MC, Barbieri L, Leonelli C. Incinerator bottom ash and ladle slag for geopolymers synthesis. Waste Biomass Valoriz. 2014;5:393–401.
15. Mahlin D, Wood J, Hawkins N, Mahey J, Royall PG. A novel powder sample holder for the determination of glass transition temperatures by DMA. Int J Pharm. 2009;371(1–2):120–5.
16. Cicala G, Mamo A, Recca G, Restuccia CL. Synthesis and thermal characterization of some novel ABA block copolymers. Macromol Mater Eng. 2007;292(5):588–97.
17. Carlier V, Sclavons M, Legras R. Supported dynamic mechanical thermal analysis: an easy, powerful and very sensitive technique to assess thermal properties of polymer, coating and even nanocoating. Polymer. 2001;42(12):5327–35.
18. Abate L, Badea E, Blanco I, Della Gatta G. Heat capacities and enthalpies of solid-solid transitions and fusion of a series of eleven primary alkylamides by differential scanning calorimetry. J Chem Eng Data. 2008;53(4):959–65.
19. Blanco I, Oliveri L, Cicala G, Recca A. Effects of novel reactive toughening agent on thermal stability of epoxy resin. J Therm Anal Calorim. 2012;108(2):685–93.
20. Vyazovkin S, Chrissafis K, Di Lorenzo ML, Koga N, Pijolat M, Roduit B, Sbirrazzuoli N, Suñol JJ. ICTAC kinetics committee recommendations for collecting experimental thermal analysis data for kinetic computations. Thermochim Acta. 2014;590:1–23.
21. Tranquillo E, Barrino F, Dal Poggetto G, Blanco I. Sol–gel synthesis of silica-based materials with different percentages of PEG or PCL and high chlorogenic acid content. Materials. 2019;12(1):155.
22. Catauro M, Dell'Era A, Vecchio Ciprioti S. Synthesis, structural, spectroscopic and thermoanalytical study of sol-gel derived SiO_2–CaO–P_2 O_5 gel and ceramic materials. Thermochim Acta. 2016;625:20–7.
23. Catauro M, Tranquillo E, Barrino F, Blanco I, Dal Poggetto F, Naviglio D. Drug release of hybrid materials containing Fe(II) citrate synthesized by sol–gel technique. Materials. 2018;11(11):2270.
24. Frost RL, Fredericks PM, Shurvell HF. Raman microscopy of some kaolinite clay minerals. Can J Appl Spectrosc. 1996;41(1):10–4.
25. Goudouri OM, Kontonasaki E, Chrissafis K, Zinn K, Hoppe A, Detsch R, Boccaccini AR. Towards the synthesis of an Mg-containing silicate glass–ceramic to be used as a scaffold for cementum/alveolar bone regeneration. Ceram Int. 2014;40(10):16287–98.
26. Roviello G, Ricciotti L, Ferone C, Colangelo F, Cioffi R, Tarallo O. Synthesis and characterization of novel epoxy geopolymer hybrid composites. Materials. 2013;6(9):3943–62.
27. Tsai YL, Hanna JV, Lee YL, Smith ME, Chan JC. Solid-state NMR study of geopolymer prepared by sol–gel chemistry. J Solid State Chem. 2010;183(12):3017–22.
28. Catauro M, Lancellotti I, Leonelli C. Addition of WEEE glass to metakaolin-based geopolymeric binder: a cytotoxicity study. Environments. 2017;4(4):89.
29. Cicala G, Recca G. Thermomechanical and morphological properties of epoxy blends with hyperbranched polyester: effect of the pseudo-generation number. J Appl Polym Sci. 2010;115(3):1395–406.
30. Cicala G, Mamo A, Recca G, Restuccia CL. Study on epoxy/thermoplastic blends based on the addition of a novel aromatic block copolymer. Polym Eng Sci. 2007;47(12):2027–33.
31. Rahier H, Van Mele B, Wastiels J. Low-temperature synthesized aluminumsilicate glasses. J Mat Sci. 1996;31:80–5.
32. Rahier H, Wastiels J, Biesemans M, Willmen R, Van Assche G, Van Mele B. Reaction mechanism, kinetics and high temperature transformations of geopolymers. J Mat Sci. 2007;42:2982–96.
33. Temuujin J, Minjigmaa A, Rickard W, van Riessen A. Thermal properties of spray-coated geopolymer-type compositions. J Therm Anal Calorim. 2012;107:287–92.
34. Fina A, Tabuani D, Carniato F, Frache A, Boccaleri E, Camino G. Polyhedral oligomeric silsesquioxanes (POSS) thermal degradation. Thermochim Acta. 2006;440:36–42.
35. Blanco I, Bottino FA, Abate L. Influence of n-alkyl substituents on the thermal behaviour of Polyhedral Oligomeric Silsesquioxanes (POSSs) with different cage's periphery. Thermochim Acta. 2016;623:50–7.
36. Singh B, Gilkes RJ. An electron optical investigation of the alteration of kaolinite to halloysite. Clays Clay Miner. 1992;40(2):212–29.
37. Catauro M, Barrino F, Dal Poggetto G, Crescente G, Piccolella S, Pacifico S. Chlorogenic acid entrapped in hybrid materials with high PEG content: a strategy to obtain antioxidant functionalized biomaterials? Materials. 2019;12(1):148.